

# **RIGHT VENTRICULAR FUNCTION AND PROGNOSIS: MOVING BEYOND CONVENTIONAL ECHOCARDIOGRAPHY**

**Ph.D. thesis**

**Máté Balázs Tolvaj, M.D.**

Semmelweis University Doctoral School  
Cardiovascular Medicine and Research Division



Supervisor: Attila Kovács, M.D., Ph.D.

Official reviewers: Csaba Jenei, M.D., Ph.D.  
Ádám Tárnoki, M.D., Ph.D.

Head of the Complex Examination Committee: Alán Alpár, M.D., D.Sc.

Members of the Complex Examination Committee: László Csernák, M.D., Ph.D.  
Róbert Langer, M.D., Ph.D.

Budapest  
2025

## **1. Introduction**

### **1.1. The forgotten chamber - historical reappraisal of right ventricular function**

The right ventricle (RV) was considered secondary to the left ventricle (LV), primarily serving as a passive conduit between the systemic venous return and the pulmonary circulation for most of the 20th century and was often overlooked in both clinical assessments and scientific research, earning it the retrospective characterization as "the forgotten chamber". This paradigm began to shift in the latter decades of the century, as accumulating clinical and experimental evidence revealed the RV's critical role in maintaining circulatory homeostasis, particularly under conditions of increased afterload such as pulmonary hypertension and left-sided heart failure.

### **1.2. The importance of right ventricular systolic function in left-sided cardiac diseases**

RV function not only has prognostic significance in pathologies primarily affecting the right heart, such as pulmonary hypertension, right-sided heart failure, congenital heart diseases, and chronic obstructive pulmonary disease (COPD), but it has also shown its critical determinant factor of clinical status and prognosis in left-sided heart failure, whether with reduced (HFrEF) or preserved ejection fraction (HFpEF). Numerous studies have demonstrated that RV dysfunction in left-sided heart failure is independently associated with increased mortality, reduced exercise capacity, and higher rates of hospitalization.

### **1.3. Conventional echocardiographic parameters of right ventricular systolic function**

Among the most widely utilized measures is tricuspid annular plane systolic excursion (TAPSE), which evaluates the longitudinal motion of the lateral tricuspid annulus toward the apex during systole. However, TAPSE is angle- and load-dependent, reflects only regional longitudinal motion, and may underestimate dysfunction in diseases with segmental wall abnormalities or altered RV geometry. RV fractional area change (FAC), which represents the percentage change in RV cavity area between diastole and systole in the apical four-chamber view, provides a two-dimensional (2D) estimate of global systolic function. While FAC captures both longitudinal and radial components of contraction, its accuracy is limited by the complex, crescent-shaped geometry of the RV, which cannot be fully appreciated in a single 2D plane. RV free wall longitudinal strain (FWLS), derived from 2D speckle-tracking echocardiography, provides a sensitive, angle-independent measure of myocardial deformation along the longitudinal axis. Nevertheless, it requires adequate image quality, is subject to vendor-specific variability (Figure 1).

#### 1.4. Three-dimensional echocardiography in right ventricular function assessment

Unlike traditional 2D methods, 3D echocardiography captures the RV's complex, crescentic geometry in its entirety. Image acquisition typically involves a full-volume and electrocardiogram-gated apical four-chamber view using a matrix-array transducer, ensuring that the entire RV cavity is enclosed within the dataset. Post-processing is performed using dedicated software platforms that allow for direct measurement of RV end-diastolic volume (EDV), end-systolic volume (ESV), stroke volume (SV), and ejection fraction (EF), without the need for geometric extrapolation (Figure 1).

#### 1.5. Three-dimensional motion decomposition of right ventricular function

The ReVISION method (Right VEntrIcular Separate wall motion quantification) is a novel 3D motion decomposition technique designed to dissect RV systolic function into its three principal components: longitudinal, radial, and anteroposterior contraction. It allows for measurement of mechanical parameters along the three axes of motion and also global strain metrics, such as global longitudinal strain (GLS) and global circumferential strain (GCS). This offers a nuanced appreciation of RV mechanics and can help identify subclinical or regional dysfunction not captured by conventional global indices (Figure 1).

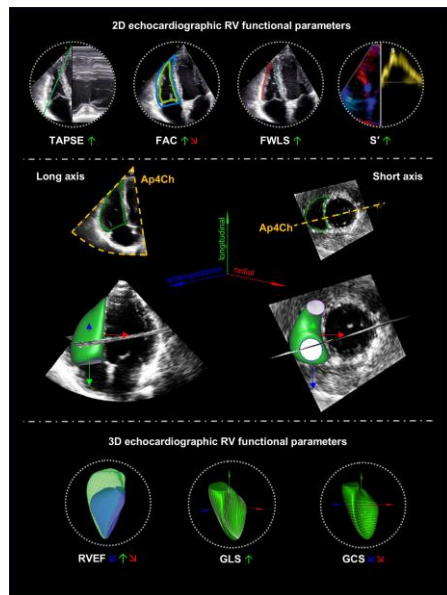


**Figure 1.** Illustration of the complex three-dimensional (3D) nature of right ventricular (RV) structure and mechanics, and the limitations of two-dimensional (2D) assessment.

## **2. Objectives**

### **2.1. Investigating the added predictive value of right ventricular ejection fraction compared with conventional echocardiographic measurements in patients who underwent diverse cardiovascular procedures**

We aimed to investigate the association between RVEF and 2-year all-cause mortality in a diverse population of patients who underwent various cardiovascular procedures at a tertiary care center, and evaluate whether RVEF outperforms conventional echocardiographic parameters in predicting outcomes.

### **2.2. Evaluating the disagreement between conventional parameters and 3D echocardiography-derived ejection fraction in the detection of right ventricular systolic dysfunction and its association with outcomes**

Conventional echocardiographic parameters such as TAPSE, FAC, and offer only a partial depiction of the complex functional attributes of the RV, whereas 3DE-derived RVEF offers a more comprehensive and integrative evaluation of RV performance. Understanding the divergence in RV systolic function classification by different approaches may substantially influence clinical decision-making, risk stratification, and prognostication. Accordingly, we sought to explore the discordance between TAPSE, FAC, FWLS, and RVEF in the evaluation of RV systolic function and its impact on clinical outcomes.

### **2.3. Assessing the prognostic significance of RV circumferential strain**

The advantages of 3DE over conventional echocardiography facilitate a more comprehensive characterization and quantification of ventricular structure and function, including the assessment of GLS and GCS for both the LV and RV. Although detailed evaluation of RV function is frequently overlooked in the context of left-sided heart diseases, the presence of RV dysfunction is associated with greater symptom burden and an elevated risk of long-term adverse outcomes. Accordingly, we aimed to evaluate LV and RV GLS and GCS using 3DE in order to determine their prognostic significance.

### **3. Methods**

#### **3.1. Study designs, populations and outcomes**

##### **3.1.1. Investigating the added predictive value of right ventricular ejection fraction compared with conventional echocardiographic measurements in patients who underwent diverse cardiovascular procedures**

Clinically and hemodynamically stable patients who underwent clinically indicated transthoracic echocardiography at the Heart and Vascular Center of Semmelweis University, Budapest, Hungary, between May 2015 and May 2019 were retrospectively identified. Inclusion criteria were: (1) age  $\geq$ 18 years; (2) established left-sided cardiac disease with previous or planned cardiac intervention or surgery, regardless of LVEF and RVEF values; (3) availability of 3DE images suitable for 3D LV and RV quantification; and (4) accessible two-year follow-up data. Patients were excluded if they had (1) primary RV pathology (e.g., primary pulmonary hypertension, arrhythmogenic cardiomyopathy, or congenital right heart disease); (2) acute cardiovascular conditions (acute coronary syndrome, myocarditis, pulmonary embolism, etc.); or (3) inadequate echocardiographic image quality. Clinical characteristics, including demographic data, medical history, physical status and vital signs, as well as laboratory parameters, were retrospectively retrieved from electronic medical records. The study was conducted in accordance with the Declaration of Helsinki and approved by the Regional and Institutional Committee of Science and Research Ethics. Follow-up data (status [dead or alive], date of death) were obtained from Hungary's National Health Insurance Database. The primary endpoint was all-cause mortality at two years.

##### **3.1.2. Evaluating the disagreement between conventional parameters and 3D echocardiography-derived ejection fraction in the detection of right ventricular systolic dysfunction and its association with outcomes**

Patients with various cardiac pathologies who underwent clinically indicated 2D and 3DE between December 2014 and March 2021 at the Department of Cardiology, Istituto Auxologico Italiano, IRCCS, Milan, Italy, and at the Heart and Vascular Center of Semmelweis University, Budapest, Hungary, were retrospectively identified.

The inclusion criteria comprised: (1) availability of both LV and RV full-volume datasets; (2) adequate image quality and volume rate enabling comprehensive LV and RV volumetric analysis; and (3) availability of follow-up data. All patients underwent standardized 2D and 3DE imaging protocols. Demographic and clinical characteristics, including age, weight, height, body surface

area (BSA), body mass index (BMI), systolic and diastolic blood pressure, heart rate, cardiovascular risk factors, comorbidities, and medical history, were extracted from the electronic clinical records. RV systolic dysfunction was defined as RVEF<45%. Guideline-recommended thresholds were applied to identify RV systolic dysfunction using conventional parameters (i.e., TAPSE <17 mm, FAC <35%, and FWLS >−20%). Written informed consent was waived due to the retrospective nature of the study. The study protocol follows the Declaration of Helsinki, and it was approved by the Semmelweis University Regional and Institutional Committee of Science and Research Ethics (approval no. 190/2020) and by the Ethics Committee of the Istituto Auxologico Italiano (approval no. 2021\_05\_18\_13). Follow-up data (status [dead or alive], date of death) were obtained from clinical records, Hungary's National Health Insurance Database, and Italy's National Health Service Database. The primary endpoint of our study was all-cause mortality.

### **3.1.3. Assessing the prognostic significance of RV circumferential strain**

Clinically and hemodynamically stable patients with an established diagnosis of left-sided cardiac disease were selected from the previously published RVENet dataset (<https://rvenet.github.io/dataset/>). This dataset includes individuals who underwent clinically indicated 2D and 3DE at the Heart and Vascular Center of Semmelweis University, Budapest, Hungary, between November 2013 and March 2021. Exclusion criteria included: (1) suspicion or presence of any primary right-sided cardiac disease at the initial report or identified during the review of the previously acquired datasets, and (2) suboptimal 3D image quality of the LV and RV datasets precluding accurate 3D analysis. Demographic and clinical data, including age, weight, height, BSA, BMI, systolic and diastolic blood pressure, heart rate, cardiovascular risk factors, comorbidities, medical history, and laboratory parameters, were obtained from electronic clinical records. Due to the retrospective nature of this analysis, obtaining written informed consent was waived. The study protocol follows the Declaration of Helsinki, and it was approved by the Semmelweis University Regional and Institutional Committee of Science and Research Ethics (approval No. 190/2020). Patients were followed for up to 6 years. Follow-up data (status [dead or alive], date of death) were obtained from Hungary's National Health Insurance Database. The primary endpoint of our study was all-cause mortality.

### **3.2. Two- and three-dimensional echocardiography**

Transthoracic echocardiographic examinations were performed using commercially available ultrasound systems (E9 and E95 with 4V-D or 4Vc-D probes, GE Vingmed Ultrasound, Horten, Norway; and EPIQ 7 with X5-1 probe, Philips Medical Systems, Best, the Netherlands). A standardized acquisition protocol was employed, incorporating 2D loops obtained from parasternal, apical, and subxiphoid views. Digitally stored raw-data sets were analyzed offline using dedicated software packages (EchoPAC BT12, GE Vingmed, Horten, Norway; and TomTec Imaging, Unterschleissheim, Germany). All parameters were assessed in accordance with current guideline recommendations. 3D datasets focused on the left heart were analyzed using semiautomated, commercially available software (AutoLVQ, EchoPAC BT12, GE Vingmed, Horten, Norway; and 4D LV-Analysis 3 and 4D RV-Function 2, TomTec Imaging, Unterschleissheim, Germany). Additionally, 3D RV GLS and GCS were quantified with the ReVISION software (Argus Cognitive, Inc., Lebanon, NH, USA).

### **3.3. Statistical analysis**

Statistical analyses were conducted using SPSS (versions 22 and 25, IBM, Armonk, NY, USA), GraphPad Prism (version 9.5.1, GraphPad Software, Inc., Boston, MA, USA), and R (version 3.6.2, R Foundation for Statistical Computing, Vienna, Austria). Continuous variables are presented as mean  $\pm$  standard deviation (SD), while categorical variables are expressed as frequencies and percentages. Normality of distribution was assessed using the Kolmogorov-Smirnov and Shapiro-Wilk tests. Clinical and echocardiographic characteristics were compared using unpaired Student's t-test or Mann-Whitney U-test for continuous variables, and Chi-squared or Fisher's exact test for categorical variables, as appropriate. For comparisons involving more than two groups, one-way ANOVA, Welch's ANOVA, or Kruskal-Wallis tests were applied for continuous variables, and  $\chi^2$  or Fisher's exact tests for categorical variables. Univariable Cox regression analysis was employed to identify factors associated with all-cause mortality. Multivariable Cox proportional hazards models were constructed and evaluated using the Akaike Information Criterion (AIC) to determine the optimal model fit. Survival curves were generated using the Kaplan-Meier method and compared via log-rank tests. Cox proportional hazards models were used to estimate hazard ratios (HRs) with corresponding 95% confidence intervals (95% CIs) between groups. To assess the prognostic performance of individual echocardiographic parameters, Harrell's C-indices (concordance indices) were compared in univariable Cox models. Receiver-operating characteristic (ROC) curves were constructed to evaluate the discriminative

capacity of different echocardiographic parameters, with optimal cut-off values determined using Youden's index. Comparisons of the areas under the ROC curves (AUCs) were performed using the DeLong test (MedCalc Statistical Software, version 22.018, MedCalc Software Ltd, Ostend, Belgium). Sankey diagrams were created using SankeyMATIC (<https://sankeymatic.com>). A two-sided P-value <0.05 was considered statistically significant.

### **3.4. Language editing**

ChatGPT (version 4.0, OpenAI, San Francisco, CA, USA) was used to improve the language of the initial draft of this thesis.

## **4. Results**

### **4.1. Investigating the added predictive value of right ventricular ejection fraction compared with conventional echocardiographic measurements in patients who underwent diverse cardiovascular procedures**

#### **4.1.1. Patient characteristics and outcomes**

The study population comprised 174 patients with a mean age of 62 years and a male predominance (72%). Among them, 78 patients (45%) had HFrEF, of whom 69 were referred to our electrophysiology department for evaluation of potential de novo device implantation or device upgrade. During follow-up, 14 patients received an implantable cardioverter defibrillator (ICD), while 49 underwent cardiac resynchronization therapy with defibrillator (CRT-D) implantation. Additionally, 9 patients were assessed for candidacy for LV assist device (LVAD) implantation; subsequently, all received the device. Twenty-eight patients (16%) were heart transplant (HTX) recipients, evaluated at a median of 96 days post-transplantation (range: 9–515 days). Sixty-eight patients (39%) presented with severe primary mitral valve regurgitation (MR; 29 with Barlow's disease and 39 with fibroelastic deficiency), enrolled in a previous prospective study, and subsequently underwent mitral valve repair or replacement following echocardiographic assessment. Over a two-year follow-up, 24 patients met the primary endpoint of all-cause mortality.

#### **4.1.2. Patients meeting vs. not meeting the endpoint**

Patients who died were older ( $68 \pm 10$  years); however, there were no significant differences in anthropometric parameters, blood pressure values, or serum creatinine levels at the time of echocardiographic assessment. Similarly, no differences were observed regarding medical

history: the prevalence of coronary artery disease, arterial hypertension, diabetes mellitus, and atrial fibrillation was comparable between the groups. Regarding conventional and 3D echocardiographic parameters, patients who died had higher LVESVi, as well as lower LVEF and LVGLS. In contrast, LVEDVi, LVSVi, and LVMi were similar between the groups. LV diastolic function parameters, including E/A and E/e' ratios, also showed no significant differences. Patients with adverse outcomes demonstrated significantly higher RVEDVi and RVESVi, while RVSVi was comparable. Among RV functional parameters, RVEF, FAC, and 2D FWLS were significantly reduced in those who died. Importantly, TAPSE and RVSP did not differ between groups.

#### **4.1.3. Univariable Cox proportional hazards models**

In univariable Cox analysis, among left-heart echocardiographic parameters, only LVEF (HR [95% CI]: 0.973 [0.950 – 0.997], p<0.05) and LVGLS (HR [95% CI]: 1.075 [1.009 – 1.146], p<0.05) were significantly associated with the primary endpoint, whereas LV volumes, LVMi, and diastolic function parameters were not. Regarding right-heart metrics, in addition to RVEDVi, RVESVi, FAC, and 2D FWLS, RVEF (HR [95% CI]: 0.945 [0.908 – 0.984], p<0.01) was significantly associated with adverse outcomes, while TAPSE and RVSP showed no association.

#### **4.1.4. Comparison of the discriminatory power by receiver-operator characteristic analysis**

Using ROC analysis, we assessed the relative discriminatory power of RV systolic function parameters (TAPSE, FAC, FWLS, RVEF) in predicting the primary endpoint. Among these, RVEF showed the highest AUC (0.679; 95% CI: 0.566–0.791) compared with the other RV functional metrics (Table 1).

**Table 1.** Receiver-operating characteristic analysis comparing the discriminatory power of right ventricular systolic function parameters concerning the primary endpoint

	AUC [95% CI]	Optimal cut-off	Sensitivity	Specificity
<b>RVEF</b>	0.679 [0.566 – 0.791]	48.2 %	0.57	0.79
<b>TAPSE</b>	0.600 [0.501 – 0.698]	24.0 mm	0.35	0.96
<b>FAC</b>	0.630 [0.495 – 0.766]	34.1 %	0.80	0.52
<b>FWLS</b>	0.643 [0.515 – 0.771]	-19.4 %	0.57	0.75

## 4.2. Evaluating the disagreement between conventional parameters and 3D echocardiography-derived ejection fraction in the detection of right ventricular systolic dysfunction and its association with outcomes

### 4.2.1. Patient characteristics and outcomes

In this two-center study, a total of 750 Caucasian patients were included (393 patients from the Department of Cardiology, Istituto Auxologico Italiano, IRCCS, Milan, Italy, and 357 patients from the Heart and Vascular Center, Semmelweis University, Budapest, Hungary). Over a median follow-up period of 3.7 years (interquartile range, 2.7–4.5 years), 112 patients (15%) died.

### 4.2.2. Patients meeting vs. not meeting the endpoint

The most prevalent comorbidities were hypertension (60%), dyslipidemia (46%), coronary artery disease (26%), and diabetes (20%). Patients who died were older, had higher heart rates, a higher prevalence of diabetes and coronary artery disease, and more frequently underwent ICD implantation; these conditions and comorbidities were also significant predictors of mortality in univariable Cox regression analysis. All assessed 2D and 3DE parameters of RV size and systolic function differed significantly between patients who stayed alive and those who died during follow-up and were similarly associated with all-cause mortality.

### 4.2.3. Comparison of right ventricular systolic function parameters

The univariable Cox model including RVEF demonstrated the highest Harrell's C-index (RVEF: 0.729 [95% CI: 0.678 – 0.780], FAC: 0.686 [95% CI: 0.631 – 0.741], FWLS: 0.688 [95% CI: 0.637 – 0.739], TAPSE: 0.664 [95% CI: 0.613 – 0.715]). When comparing the C-indices, RVEF showed significantly superior prognostic power compared to FWLS ( $p=0.029$ ) and TAPSE ( $p=0.035$ ), whereas no significant difference was observed compared to FAC ( $p = 0.130$ ). The HRs of the parameters dichotomized according to guideline-defined cut-off values are presented in Table 2. The greatest increase in the risk of all-cause mortality was identified when RV dysfunction was defined by RVEF (HR [95% CI]: 4.676 [3.169 – 6.900],  $p<0.001$ ).

**Table 2.** Hazard ratios of the parameters dichotomized based on the guideline-defined cut-off values

Univariable Cox proportional-hazards models		
	HR [95% CI]	p
RVEF<45%	4.676 [3.169 – 6.900]	<0.001
TAPSE<17 mm	2.824 [1.939 – 4.113]	<0.001
FAC<35%	3.044 [2.032 – 4.559]	<0.001
FWLS>-20%	2.569 [1.767 – 3.736]	<0.001

FWLS demonstrated the highest discriminatory power (AUC: 0.877 [95% CI: 0.852 – 0.902,  $p<0.001$ ]) for identifying RV systolic dysfunction (defined as RVEF<45%), surpassing that of FAC (AUC: 0.787 [95% CI: 0.750 – 0.824,  $p<0.001$ ]) and TAPSE (AUC: 0.729 [95% CI: 0.690 – 0.767,  $p<0.001$ ]) (Figure 2). Significant differences were observed among all AUCs based on DeLong tests (FAC vs. FWLS  $p<0.001$ ; FAC vs. TAPSE  $p=0.015$ ; FWLS vs. TAPSE  $p<0.001$ ). According to guideline-recommended cut-off values, the sensitivity and specificity for detecting RV systolic dysfunction (RVEF<45%) were 55% and 79% for TAPSE, 76% and 67% for FAC, and 59% and 92% for FWLS, respectively, as determined by ROC analysis.

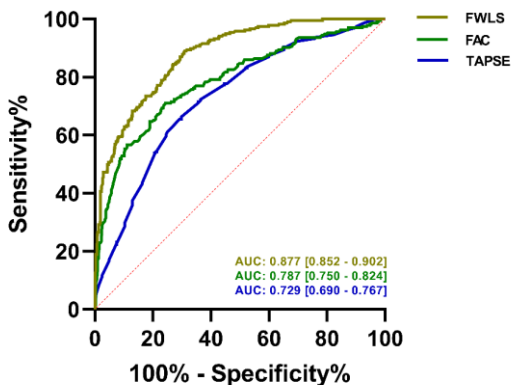


**Figure 2.** Receiver operating characteristic (ROC) curves of the conventional parameters for the discrimination of RV systolic dysfunction (RVEF<45%) with corresponding area under the curve (AUC) values.

#### 4.2.4. Multiparametric assessment of right ventricular systolic function using conventional parameters

Clinical outcomes were the worst if at least two conventional echocardiographic parameters indicated RV systolic dysfunction, and progressively improved when only one or none of these parameters was abnormal. All Kaplan-Meier curves differed significantly from each other (log-rank  $p<0.005$ ), except for the comparison between the curves representing two versus three impaired parameters (Figure 3).

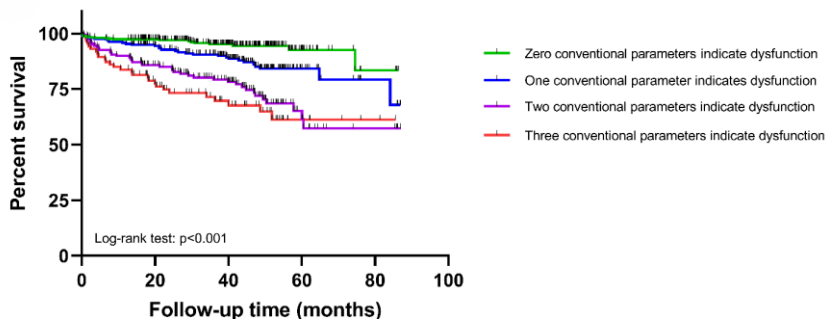


**Figure 3.** Survival analysis of patients divided into subgroups based on the number of conventional parameters indicating RV dysfunction. The survival of patients is visualized via Kaplan-Meier curves with the P-value of the overall log-rank test.

The risk of death more than doubled (HR [95% CI]: 2.176 [1.348 – 3.511], p=0.001) when two conventional parameters indicated dysfunction, and nearly tripled (HR [95% CI]: 2.890 [1.707 – 4.891], p<0.001) when three parameters indicated dysfunction, compared with cases in which only one parameter indicated dysfunction. To identify the most effective pair of conventional parameters for combined assessment, we calculated the HRs for all three possible parameter combinations. The combination of FAC and FWLS indicating RV dysfunction exhibited the highest HR compared to cases with zero parameters indicating dysfunction (HR [95% CI]: 5.841 [2.107 – 16.190], p=0.001).

However, log-rank tests showed no significant differences between the Kaplan-Meier curves of any two-parameter combinations and those of the subgroup with all three parameters indicating dysfunction (Figure 4).

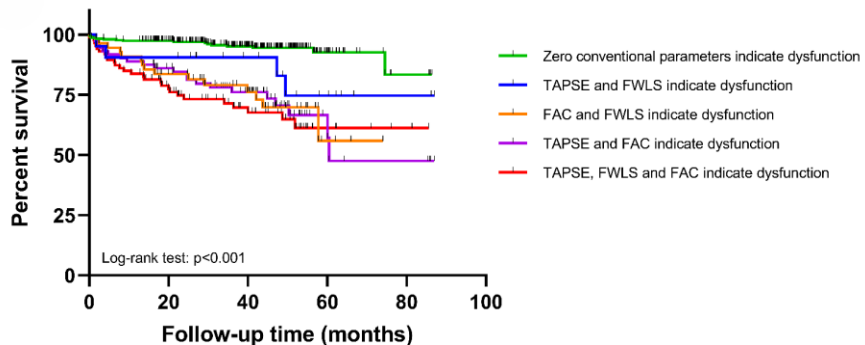


**Figure 4.** Survival analysis of patients divided into subgroups based on the two-parameter combinations of conventional parameters indicating RV dysfunction. The survival of patients is visualized via Kaplan-Meier curves with the *p*-value of the overall log-rank test.

There were also no significant differences between the Kaplan-Meier curves when the subgroups were defined by the presence of RV dysfunction indicated by any two conventional parameters, regardless of the value of the third parameter.

#### 4.2.5. Reclassification of right ventricular systolic function by ejection fraction

##### 4.2.5.1. Reclassification in the full cohort

In total, 511 patients (68%) exhibited normal RV function when assessed by RVEF. Although an equivalent number of patients were classified as having normal RV function using TAPSE, 21% of these demonstrated impaired RVEF. When using FAC, only 404 patients were categorized as having preserved RV function; however, 15% of this subgroup had RV dysfunction according to RVEF. In contrast, FWLS identified 567 patients without dysfunction, yet 17% of these were reclassified as having RV dysfunction based on RVEF (Figure 5). Conversely, RV dysfunction was identified in 239 patients (32%) based on RVEF. While TAPSE classified an identical number of patients as having dysfunction, 46% of these were misclassified relative to RVEF. Using FAC, 346 patients were assigned to the dysfunction group; however, 49% of these did not exhibit dysfunction according to RVEF. In contrast, FWLS identified 183 patients with RV dysfunction, with 23% subsequently reclassified as having preserved function when evaluated by RVEF.

## Full cohort

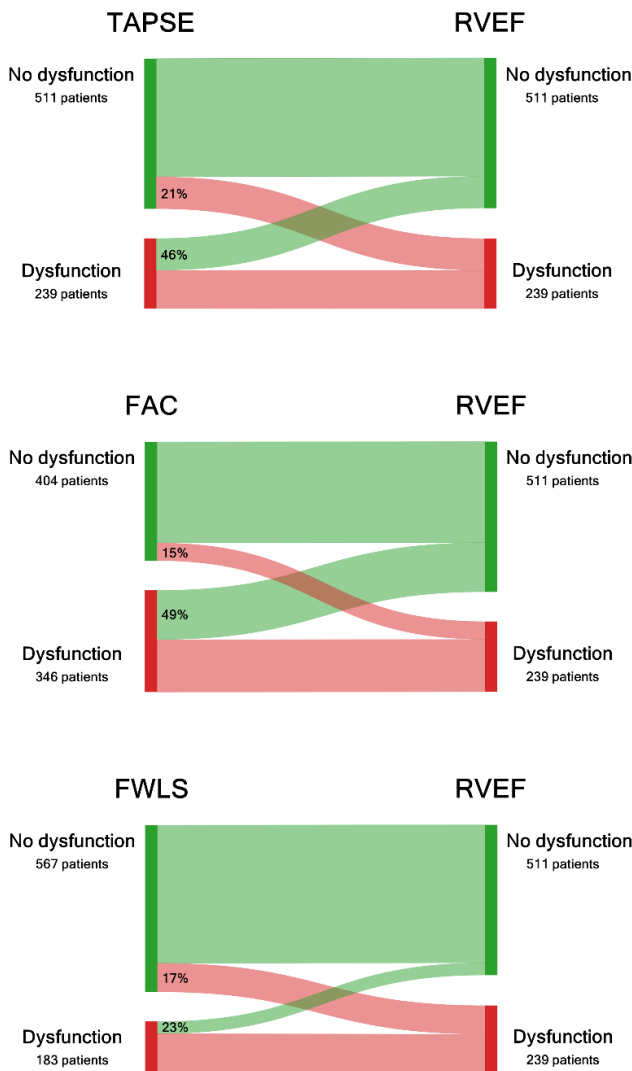


**Figure 5.** Disagreement in the classification of RV systolic function between conventional parameters and 3DE-derived RVEF, visualized on Sankey diagrams.. Green flows represent patients without RV dysfunction, and red flows represent patients with RV dysfunction by RVEF.

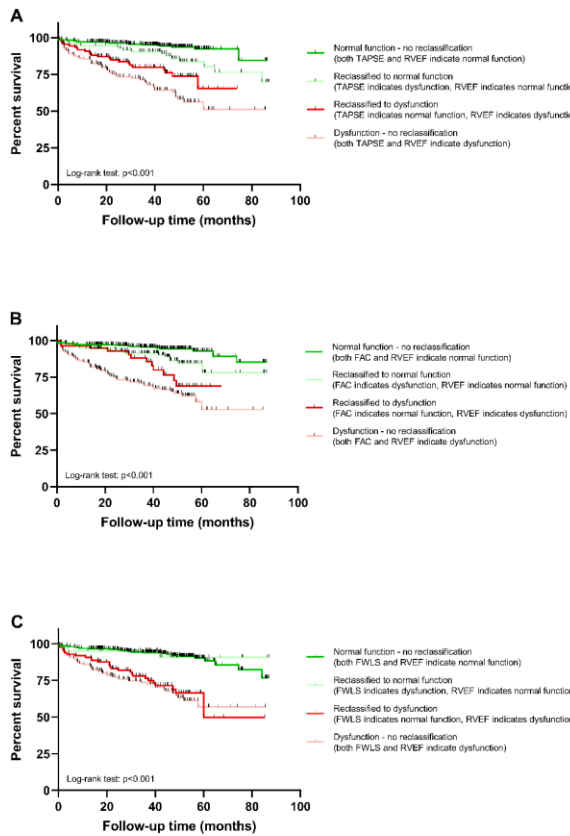


**Figure 6.** Survival analysis of patients divided into subgroups based on the combination of different parameters detecting right ventricular systolic dysfunction. The survival of patients is visualized via Kaplan-Meier curves with the  $p$ -value of the overall log-rank test. Green and red colors with the same opacity were used to indicate subgroups that were compared due to reclassification based on RVEF.

To further clarify the clinical significance of RVEF-based reclassification, outcomes were compared between reclassified and non-reclassified patients (Figure 6). Patients with normal conventional parameters who were reclassified as having RV dysfunction exhibited a more than four-fold increased risk of mortality compared to those not reclassified (TAPSE HR [95% CI]: 4.395 [2.127 – 9.085],  $p<0.001$ ; FAC HR [95% CI]: 4.186 [1.476 – 11.880],  $p<0.001$ ; FWLS HR [95% CI]: 4.221 [2.115 – 8.426],  $p<0.001$ ). Conversely, patients with abnormal conventional

parameters who were reclassified as having normal RV function demonstrated a substantially lower mortality risk relative to non-reclassified patients (TAPSE HR [95% CI]: 0.326 [0.199 – 0.532],  $p < 0.001$ ; FAC HR [95% CI]: 0.308 [0.197 – 0.480],  $p < 0.001$ ; FWLS HR [95% CI]: 0.195 [0.102 – 0.373],  $p = 0.002$ ). Importantly, however, there was an added mortality risk in those subgroups where RVEF was normal, but TAPSE or FAC was abnormal compared to those subgroups in which both RVEF and TAPSE or FAC were within normal ranges (TAPSE HR [95% CI]: 2.111 [1.041 – 4.280]  $p = 0.014$ , FAC HR [95% CI]: 2.237 [1.142 – 4.384]  $p = 0.010$ ).

#### **4.2.5.2. Subgroup analysis**

The study cohort was categorized into the following clinical subgroups: aortic valve disease (n=120, 16%), mitral valve disease (n=108, 14%), HTX (n=91, 12%), non-ischemic dilated cardiomyopathy (DCM) (n=88, 12%), ischemic cardiomyopathy (n=76, 10%), acute coronary syndrome (ACS) (n=82, 11%), other cardiomyopathy (n=31, 4%) and a heterogeneous subgroup comprising various other cardiac diseases (n=154, 21%). Regarding the subgroups' classification based on TAPSE, the highest reclassification rate was observed among HTX patients (71%), followed by those with ischemic cardiomyopathy (32%), non-ischemic DCM (31%), aortic valve disease (25%), ACS (21%), and mitral valve disease (17%). When RV function was evaluated using FAC, reclassification was observed in 51% of patients with mitral valve disease, 40% of HTX patients, 30% of those with non-ischemic DCM, 28% with ischemic cardiomyopathy, 25% with aortic valve disease, and 17% with ACS. The evaluation based on FWLS demonstrated comparable or lower rates of reclassification relative to other conventional functional parameters. Specifically, reclassification occurred in 28% of patients with ischemic cardiomyopathy, 20% in those with non-ischemic DCM and aortic valve disease, 19% in the HTX subgroup, 17% in the ACS subgroup, and 13% among patients with mitral valve disease.

### **4.3. Assessing the prognostic significance of RV circumferential strain**

#### **4.3.1. Patient characteristics and outcomes**

A total of 357 patients (age:  $64 \pm 15$  years, 70% male) with established left-sided cardiac disease and 3DE recordings of suitable quality for both LV and RV analysis were identified from the RVENet dataset, including HFrEF (27%), severe MR (19%), aortic stenosis (22%) and atrial fibrillation (7%) patients later undergoing procedure and HTX recipient (26%) evaluated at a median of 157 days post-transplantation. Over a median follow-up time of 41 months (interquartile range 20–52), 55 (15%) patients died.

#### 4.3.3. Echocardiographic characteristics

Right atrial size was larger in those patients who died, accompanied by more pronounced impairment of RV longitudinal function, as reflected by reduced TAPSE and FWLS; however, RVSP and FAC were similar. Regarding 3DE parameters, patients who died exhibited larger LV and RV volumes, as well as more severely impaired systolic function. Both LV and RV GLS and GCS were more impaired in patients who died (Table 3).

**Table 3.** 3D echocardiographic parameters

	Overall (n=357)	Alive (n=302)	Dead (n=55)	p
<b>Left ventricle</b>				
<b>LVEDVi (ml/m<sup>2</sup>)</b>	82.2±32.2	80.3±32.3	91.9±30.3	<b>0.019</b>
<b>LVESVi (ml/m<sup>2</sup>)</b>	44.5±30.4	42.2±30.0	56.3±30.0	<b>0.003</b>
<b>LVSVi (ml/m<sup>2</sup>)</b>	37.7±14.6	38.1±15.1	35.6±11.2	0.269
<b>LVMi (g/m<sup>2</sup>)</b>	102.5±36.8	100.4±35.1	113.4±43.0	<b>0.023</b>
<b>LVEF (%)</b>	49.0±15.7	50.2±15.3	42.3±16.1	<b>0.001</b>
<b>LVGLS (%)</b>	-15.2±6.0	-15.7±5.9	-12.5±6.2	<b>&lt;0.001</b>
<b>LVGCS (%)</b>	-23.9±9.1	-24.6±9.0	-20.2±9.3	<b>0.001</b>
<b>Right ventricle</b>				
<b>RVEDVi (ml/m<sup>2</sup>)</b>	70.2±23.5	68.9±23.1	76.6±24.6	<b>0.033</b>
<b>RVESVi (ml/m<sup>2</sup>)</b>	37.4±18.7	36.0±17.8	44.4±21.3	<b>0.003</b>
<b>RVSVi (ml/m<sup>2</sup>)</b>	32.7±9.0	32.8±9.3	32.2±7.5	0.648
<b>RVEF (%)</b>	48.3±9.4	49.1±9.2	44.1±9.5	<b>&lt;0.001</b>
<b>RVGLS (%)</b>	-16.4±5.1	-16.9±5.0	-13.8±4.6	<b>&lt;0.001</b>
<b>RVGCS (%)</b>	-17.7±6.1	-18.3±5.9	-14.3±6.2	<b>&lt;0.001</b>

Continuous variables are presented as means ± SD, categorical variables are reported as frequencies (%).

#### 4.3.4. Multivariable Cox regression models

Using univariable Cox regression, we identified variables associated with all-cause mortality. Subsequently, we constructed multiple multivariable Cox models, each incorporating a maximum of five predictors, by sequentially adding covariates to a baseline model (Figure 7). This approach involved three consecutive steps. In the first step, we established a baseline model (Model 0) that included age, sex, and serum creatinine level, as the latter emerged as a significant predictor in the univariable analysis. In the second step, we individually added LVEF, LVGLS, or LVGCS to this baseline model, resulting in Models 1, 2, and 3, respectively. Among these, the model incorporating LVGLS (Model 2) demonstrated the lowest AIC value (Figure 7A).

In the third step, we further refined the analysis by adding RVEF, RVGLS, or RVGCS to Model 2, yielding Models 4, 5, and 6, respectively. Of these, the model containing RVGCS (Model 6) exhibited the lowest AIC (Figure 7B). In this final model, age and RVGCS emerged as

independent predictors of all-cause mortality, whereas sex, serum creatinine level, and LVGLS did not demonstrate independent prognostic significance (Table 4).

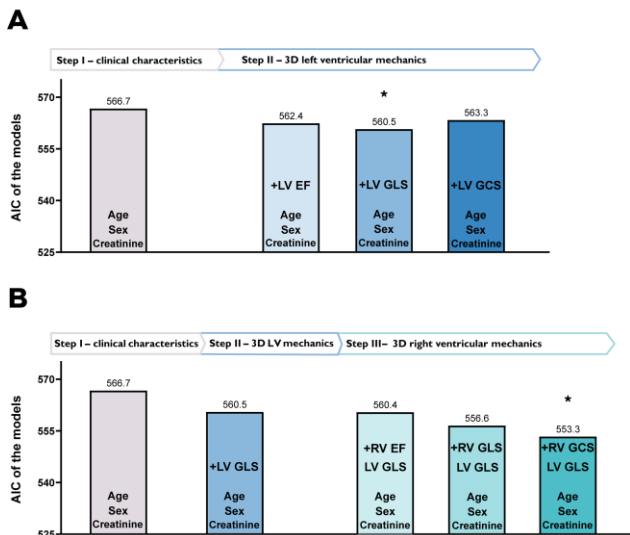


**Figure 7.** Identification of the best-fit models, including left (LV) and right ventricular (RV) functional parameters by multivariable Cox regression analysis based on Akaike Information Criterion (AIC).

**Table 4.** Independent predictors of all-cause mortality identified using multivariable Cox regression

Multivariable Cox regression		
	HR [95% CI]	p
Age	1.036 [1.011-1.061]	<b>0.004</b>
Sex	0.690 [0.376-1.266]	0.231
Creatinine	1.005 [0.999-1.012]	0.087
LVGLS	1.017 [0.963-1.075]	0.543
RVGCS	1.091 [1.032-1.152]	<b>0.002</b>

**4.3.5. Comparison of the discriminatory power by receiver-operator characteristic analysis**  
 On ROC analysis, LVGLS demonstrated the highest discriminative power among LV functional parameters (area under the ROC curve: 0.644 [95% CI: 0.561 – 0.726,  $p<0.001$ ]). Nevertheless, RVGCS exhibited the highest discriminative power among all evaluated 2D and 3D echocardiographic parameters (0.690 [95% CI: 0.614 – 0.765,  $p<0.001$ ]).

#### 4.3.6. Subgroup analysis

As the model incorporating LVGLS and RVGCS was identified as the optimal model among those evaluated, we stratified patients into four subgroups based on the median values of LVGLS ( $-15.9\%$ ) and RVGCS ( $-17.9\%$ ). Group 1 comprised patients with both LVGLS and RVGCS above the median, whereas Group 4 included patients with both parameters below the median. Group 2 consisted of patients with LVGLS below the median and RVGCS above the median, while Group 3 included those with LVGLS above the median and RVGCS below the median (Figure 8). In Group 1, 7.2% of patients died during the follow-up period, whereas in Group 2, the mortality rate was 7.5%. In contrast, adverse outcomes were more frequent in Groups 3 and 4, with mortality rates of 20.3% and 24.8%, respectively. These differences in survival among the subgroups were illustrated using Kaplan-Meier curves (Figure 9).

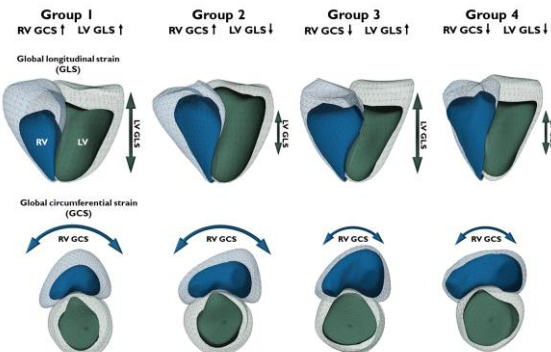


**Figure 8.** Three-dimensional schematic models depict representative cases of different biventricular mechanical patterns in patients from the respective groups.

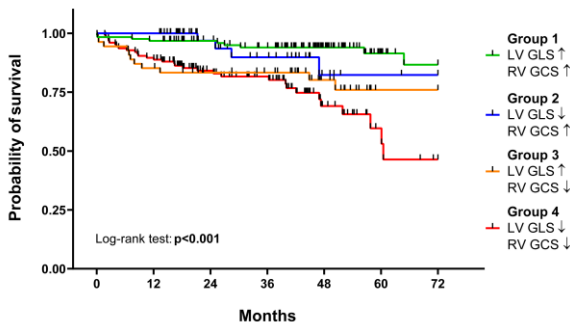


**Figure 9.** The survival of the four groups is visualized on Kaplan-Meier curves, and the log-rank test was performed for comparison.

Patients with both LVGLS and RVGCS below the median (Group 4) exhibited a more than fivefold increased risk of death compared with those in Group 1 and more than a threefold higher risk compared with Group 2. Interestingly, no significant difference in mortality was observed between Group 3 (with LVGLS above the median) and Group 4, but being categorized into Group 3 vs. Group 1 still held a more than 3-fold risk.

## 6. Conclusions

In our first study, we examined a heterogeneous cohort of patients receiving tertiary cardiology care and undergoing various cardiac procedures. We demonstrated that RVEF measured by 3DE is significantly associated with 2-year all-cause mortality and outperforms conventional RV functional parameters in predicting adverse outcomes. These findings support the routine clinical implementation of 3DE, as it offers valuable incremental information for both diagnostic and prognostic purposes. Nevertheless, larger-scale studies in more specific patient populations are needed to further delineate the utility of RVEF measurement in predicting diverse clinical endpoints and long-term outcomes.

In our second study, we found that guideline-recommended cut-off values for conventional echocardiographic parameters of RV systolic function exhibited only a modest association with RVEF as assessed by 3DE, and the extent of RV function reclassification varied according to the specific parameter employed and the underlying pathology. Among these, impaired FWLS demonstrated the strongest concordance with the RVEF cut-off. When 3DE evaluation is not feasible, a multiparametric approach to RV systolic function assessment is preferable. Notably, the presence of two or more conventional parameters indicating RV systolic dysfunction was associated with the poorest clinical outcomes.

Regarding our third study, RV circumferential shortening was shown to possess significant prognostic value for adverse clinical outcomes. RVGCS emerged as a robust and independent predictor of all-cause mortality in patients with left-sided cardiac disease. These findings underscore the clinical relevance of 3DE-derived myocardial mechanics parameters.

## 9. Bibliography of the candidate's publications

### 9.1. Bibliography related to the present thesis

1. **M. Tolvaj**, M. Tokodi, B. Lakatos, A. Fábián, A. Ujvári, F. Bakija, Z. Ladányi, Z. Tarcza, B. Merkely, A. Kovács (2021) Added predictive value of right ventricular ejection fraction compared with conventional echocardiographic measurements in patients who underwent diverse cardiovascular procedures. IMAGING, doi:10.1556/1647.2021.00049 IF: **0**
2. **M. Tolvaj\***, A. Kovács\*, N. Radu, A. Casella, D. Muraru, B. Lakatos, A. Fábián, M. Tokodi, M. Tomaselli, M. Gavazzoni, F. Perelli, B. Merkely, L. Badano, E. Surkova (2024) Significant Disagreement Between Conventional Parameters and 3D Echocardiography-Derived Ejection Fraction in the Detection of Right Ventricular Systolic Dysfunction and Its Association With Outcomes. J Am Soc Echocardiogr, doi: 10.1016/j.echo.2024.04.005. IF: **6.0** \*M. Tolvaj and A. Kovács are joint first authors.
3. **M. Tolvaj**, A. Fábián, M. Tokodi, B. Lakatos, A. Assabiny, Z. Ladányi, K. Shiida, A. Ferencz, W. Schwertner, B. Veres, A. Kosztin, Á. Szijártó, B. Sax, B. Merkely, A. Kovács (2023) There is more than just longitudinal strain: Prognostic significance of biventricular circumferential mechanics. Front Cardiovasc Med, doi: 10.3389/fcvm.2023.108275. IF: **2.8**

### 9.2. Bibliography not related to the present thesis

1. M. Tokodi, B. Magyar, A. Soós, M. Takeuchi, **M. Tolvaj**, et. al (2023) Deep Learning-Based Prediction of Right Ventricular Ejection Fraction Using 2D Echocardiograms. JACC Cardiovasc Imaging doi: 10.1016/j.jcmg.2023.02.017. IF: **12.8**
2. Á. Szijártó, A. Fábián, B. Lakatos, **M. Tolvaj**, et. al (2023) A machine learning framework for performing binary classification on tabular biomedical data. IMAGING, doi:10.1556/1647.2023.00109 IF: **0.7**
3. B. Edvi, A. Assabiny, T. Teszák, **M. Tolvaj**, et. al (2024) Trajectory of Diastolic Function after Heart Transplantation as Assessed by Left Atrial Deformation Analysis. Diagnostics, doi: 10.3390/diagnostics14111136. IF: **3.3**
4. Z. Ladányi, A. Eltayeb, A. Fábián, A. Ujvári, **M. Tolvaj**, et. Al (2024) The effects of mitral stenosis on right ventricular mechanics assessed by three-dimensional echocardiography. Sci Rep., doi: 10.1038/s41598-024-68126-y. IF: **3.9**
5. **M. Tolvaj**, F. Bakija, A. Fábián, et. al (2025) Integrating Left Atrial Reservoir Strain Into the First-Line Assessment of Diastolic Function: Prognostic Implications in a Community-Based Cohort With Normal Left Ventricular Systolic Function. J Am Soc Echocardiogr, doi: 10.1016/j.echo.2025.03.012 IF (2024): **6.0**
6. Á. Szijártó, B. Merkely, A. Kovács, M. Tokodi on behalf of the **QUEST-EF Investigators** (2025) Deep learning-enabled echocardiographic assessment of biventricular ejection fractions: the dual-task QUEST-EF model. Eur. Heart J. Cardiovasc. Imaging., doi: 10.1093/ehjci/jeaf147
7. F. Bakija, **M. Tolvaj**, Á. Szijártó, et al. (2025) Long-term prognostic value of myocardial work analysis across obesity stages: insights from a community-based study. Int. J. Obes., doi: 10.1038/s41366-025-01863-w IF (2024): **3.8**